*Virtual and Physical Prototyping*
2012, 1–10, iFirst article

Taylor & Francis
Taylor & Francis Group

# Directed cell growth and alignment on protein-patterned 3D hydrogels with stereolithography

Vincent Chan[a,d†], Mitchell B. Collens[a,d†], Jae Hyun Jeong[b], Kidong Park[c,d], Hyunjoon Kong[b] and Rashid Bashir[a,c,d*]

[a]Department of Bioengineering, University of Illinois at Urbana-Champaign, Urbana, Illinois, 61801, USA
[b]Department of Chemical and Biomolecular Engineering, University of Illinois at Urbana-Champaign, Urbana, Illinois, 61801, USA
[c]Department of Electrical and Computer Engineering, University of Illinois at Urbana-Champaign, Urbana, Illinois, 61801, USA
[d]Micro and Nanotechnology Laboratory, University of Illinois at Urbana-Champaign, Urbana, Illinois, 61801, USA

(*Received 2 July 2012; final version received 3 July 2012*)

The stereolithography apparatus (SLA) is a computer-assisted, three-dimensional (3D) printing system that is gaining attention in the medical field for the fabrication of patient-specific prosthetics and implants. An attractive class of implantable biomaterials for the SLA is photopolymerisable hydrogels because of their resemblance to soft tissues and intrinsic support of living cells. However, most laser-based SLA machines lack the minimum feature size required to imitate cell growth and alignment patterns in complex tissue architecture. In this study, we demonstrate a simple method for aligning cells on 3D hydrogels by combining the micro-contact printing (μCP) technique with the stereolithographic process. Fibronectin modified with acrylate groups was printed on glass coverslips with unpatterned, 10, 50, and 100 μm wide line patterns, which were then transferred to hydrogels through chemical linkages during photopolymerisation. Fibroblasts cultured on protein-printed 3D hydrogels aligned in the direction of the patterns, as confirmed by fast Fourier transform and cell morphometrics.

*Keywords:* stereolithography; micro-contact printing; hydrogels; cell alignment

## 1. Introduction

The stereolithography apparatus (SLA) is a computer-assisted, three-dimensional (3D) printing system used for creating complex structures from photopolymerisable resins (Jacobs 1992). Traditionally, it is a manufacturing technique intended to produce 3D models and prototypes, but practitioners in the medical field have embraced it as a way to develop custom end-use parts and preoperative surgical plans (Barker *et al*. 1994, Winder and Bibb 2005). The SLA and other 3D printing platforms have greatly improved the performance and fit of prosthetics and implants in combination with computed tomography (CT) or magnetic resonance imaging (MRI) technologies (Melchels *et al*. 2012). Fabricated parts from the SLA have been implanted as scaffolding for bone ingrowth (Cooke *et al.* 2003, Seitz *et al.* 2005), moulds for breast reconstruction (Melchels *et al*. 2011), replicas for aortic heart valves (Sodian *et al.* 2002), and shells for 'in-the-ear' hearing aids.

In the past few years, photopolymerisable hydrogels have been explored in the SLA as a potential class of implantable,

*Corresponding author. Email: rbashir@illinois.edu
†Both authors contributed equally for this study.

*Virtual and Physical Prototyping*
ISSN 1745-2759 print/ISSN 1745-2767 online 
http://www.tandfonline.com
http://dx.doi.org/10.1080/17452759.2012.709423

soft materials (Melchels *et al.* 2010). Hydrogels, which are networks of cross-linked polymers that imbibe large amounts of water, can be used directly with living cells as a synthetic extracellular matrix (ECM) analog for providing a variety of physical, chemical, and biological cues (Nguyen and West 2002, Ifkovits and Burdick 2007, Tibbitt and Anseth 2009, Jabbari 2011). In contrast to stiff 2D substrates made of polystyrene or glass, hydrogels possess 3D architecture and have tunable elasticity similar to tissues and organs. Cell attachment (Nguyen and West 2002, Hadjipanayi *et al.* 2009, Guillame-Gentil *et al.* 2010), spreading (Wong *et al.* 2004, Discher *et al.* 2005, Bott *et al.* 2010), communication (Reinhart-King *et al.* 2008, Geiger *et al.* 2009, Buxboim *et al.* 2010), and differentiation of stem cells (Discher *et al.* 2005, Engler *et al.* 2006, Vogel and Sheetz 2006) are a few of the physical effects of matrix elasticity.

Poly(ethylene glycol) diacrylate (PEGDA) is the most commonly used photopolymerisable hydrogel in the SLA. Using the working curve equation (Jacobs 1992), PEGDA with varying molecular weights was characterised for building complex 3D structures (Arcaute *et al.* 2006). Living cells encapsulated in PEGDA ($\geq M_W$ 1,000 $g \cdot mol^{-1}$) survived the stereolithographic process and remained viable within the hydrogel for up to two weeks (Chan *et al.* 2010). Integrating living cells with PEGDA hydrogels patterned in the SLA offers exciting new possibilities for tissue engineering and the development of cellular systems. For example, the SLA was used to examine cell interactions of co-cultures, such as neurons and muscle cells, encapsulated in discrete spatial locales in the same 3D construct (Zorlutuna *et al.* 2011). In another example, geometric patterns of hydrogels defined in the SLA were used to localise gradients of angiogenic growth factors secreted by encapsulated fibroblasts. When implanted *in vivo* on a vascular membrane, new blood vessels sprouted on the membrane in the same pattern as the hydrogel (Jeong *et al.* 2012). Furthermore, the SLA was modified for applications using multiple materials, such as hydrogel cantilevers and actuators that mimic the elasticity of the native myocardium for contractile muscle cells (Chan *et al.* 2012).

Despite recent progress, the SLA is limited to minimum feature sizes that are dependent on the diameter of the laser beam. Commercial SLA systems utilise gas or solid-state lasers that have a spot size between 75 and 250 μm. This limits the ability of researchers interested in creating patterns that control cell growth and alignment to imitate the *in vivo* tissue architecture. Distinct patterns are seen throughout the body, such as complex neural networks in the brain and linear arrangement of muscle cells around the myocardium (McDevitt *et al.* 2002). Protein immobilisation for patterning has been shown on and in hydrogels (Khetan and Burdick 2011) using thiol chemistry and two-photon irradiation (Lee *et al.* 2008, West 2011), and photolithography. Additionally, cell patterning has been shown mechanically by creating grooves (Charest *et al.* 2006, Park *et al.* 2006, Kim *et al.* 2007, Aubin *et al.* 2010), microchannels (Sarig-Nadir *et al.* 2009), and geometric restrictions (Parker *et al.* 2002, Aubin *et al.* 2010); however, these methods can alter material properties and mechanics which are important to maintain for specific applications.

In this current study, we exploited the cells' dependence on ECM molecules to control their growth, organisation, and distribution. Specifically, we have developed a simple method to align cells on structures fabricated using the SLA by first stamping polydimethylsiloxane (PDMS) patterns of acryl-fibronectin with micro-contact printing (μCP) and transferring the patterns to hydrogels fabricated in the SLA. This technique can then be used to align living cells on 3D hydrogel geometries, including neurons, muscle cells, and endothelial cells. From a biological perspective, the elastic properties of hydrogels combined with the ability to align cells allows for realistic *in vitro* models for understanding the biology of cell development, organisation, and disease. From an engineering perspective, using the SLA to create geometrically-defined, biohybrid constructs generates exemplary new applications in tissue engineering, regenerative medicine, synthetic biology, and cellular machines.

## 2. Materials and methods

### 2.1 *Preparation of PDMS stamp*

Master moulds for the PDMS stamps were fabricated on a silicon wafer with SU-8 negative photoresist following a standard procedure (Chen *et al.* 1998, Kane *et al.* 1999). The master moulds contained patterns of 10, 50, and 100 μm wide lines with equal spacing. The height of each pattern was 5 μm. The patterned master moulds were silanised with (tridecafluoro-1,1,2,2-tetrahydrooctyl)-1-trichlorosilane in vacuum for 1 hour. PDMS (Dow Corning Sylgard 184 Silicone Elastomer Kit) was weighed out at a 10:1 ratio of polymer-to-curing agent (heat activated). The materials were thoroughly mixed for 3 minutes to ensure even distribution of the curing agent and poured onto the patterned master moulds. Samples were placed in a desiccator, pulled under vacuum, and baked at 80 °C overnight.

### 2.2 *Preparation of fibronectin and acryl-fibronectin ink*

Fibronectin from bovine plasma solution (Sigma Aldrich, St. Louis, MO, USA) was diluted in phosphate buffer solution (PBS) to a concentration of 50 μg $mL^{-1}$. For acryl-fibronectin ink, monoacrylated poly(ethylene glycol)-*N*-hydroxysuccinimide (acryl-PEG-NHS, $M_W$ 3500 $g \cdot mol^{-1}$, JenKem Technology, Allen, TX, USA) was dissolved in PBS at a concentration of 30 mg $mL^{-1}$. A working solution of acryl-fibronectin ink was prepared by mixing acryl-PEG-NHS with fibronectin at a 2:1 molar ratio

of acrylate-to-lysine. Acryl-PEG-NHS reacts spontaneously with primary amines on the fibronectin and releases *N*-hydroxysuccinimide to form a covalent bond. The reaction was allowed to proceed for 30 minutes at 4 °C.

### 2.3 *Micro-contact printing ink on glass coverslips*

Glass coverslips were patterned by μCP (Chen *et al.* 1998, Kane *et al.* 1999) using clean PDMS stamps. Fibronectin and acryl-fibronectin ink (50 μg $mL^{-1}$) were coated onto PDMS stamps for one hour at 37 °C. After incubation, excess ink was aspirated and dried under a stream of $N_2$. Stamps were placed pattern-side down onto 18 $mm^2$ glass coverslips. Pressure was applied for 30 s to allow adsorption of ink to the glass, and the coverslips were incubated for 45 minutes. Stamps were removed, and the coverslips were used within one hour.

### 2.4 *Preparation of hydrogel pre-polymer solution*

Hydrogel pre-polymer solutions were prepared by dissolving 20% poly(ethylene glycol) diacrylate (PEGDA, $M_W$ 3400 $g \cdot mol^{-1}$, Laysan Bio, Arab, AL USA) in PBS. The photoinitiator, 1-[4-(2-hydroxyethoxy)-phenyl]-2-hydroxy-2-methyl-1-propane-1-one (Irgacure 2959, Ciba, Basel, Switzerland), was diluted to a 50% (w/v) stock solution in dimethyl sulfoxide (DMSO, Fisher Scientific). A final concentration of 0.5% (w/v) was added to the pre-polymer solution. All materials were prepared immediately before photopolymerisation in the SLA.

### 2.5 *Fabrication of photopolymerisable hydrogels*

Hydrogel constructs were fabricated with a modified stereolithography apparatus (SLA 250/50, 3D Systems, Rock Hill, SC) (Chan *et al.* 2010). Cylindrical disks (5 mm radius) were designed in AutoCAD 2012 (Autodesk, San Rafael, CA USA) and prepared in 3D Lightyear v1.4 software (3D Systems, Rock Hill, SC) for cross-sectional slicing into 2D layers. Parameters were specified based on desired layer thickness. An 18 $mm^2$ glass coverslip with unpatterned and patterned lines of fibronectin or acryl-fibronectin ink 10, 50, or 100 μm wide was fixed to a 35 mm polystyrene dish with double-sided tape. Surfaces with no patterns were always used as controls. The dish was coated with hydrogel pre-polymer solution at a characterised volume determined by desired layer thickness. It was positioned at the centre of the SLA platform and photopolymerised with a characterised energy dose of 150 mJ $cm^{-2}$. After photopolymerisation, disks were rinsed in PBS and allowed to swell overnight before cell seeding.

### 2.6 *Cell culture*

NIH/3T3 mouse embryonic fibroblasts (ATCC, Manassas, VA USA) were cultured at 37 °C and 5% $CO_2$ in Dulbecco's modified Eagle medium (DMEM, Cellgro, Manassas, VA USA) supplemented with 10% foetal bovine serum (FBS, Sigma-Aldrich, St. Louis, MO USA), 100 IU penicillin, and 100 μg $ml^{-1}$ streptomycin (Gibco, Carlsbad, CA USA). Cells were passaged no more than 10 times using 0.25% trypsin and 0.04% ethylenediaminetetraacetic acid (EDTA) in Hank's balanced salt solution (HBSS) (Gibco, Carlsbad, CA USA). Prior to cell seeding, hydrogel constructs were positioned in 12-well plates with fibronectin and acryl-fibronectin patterns facing up. Cells were then seeded at a density of 90,000 cells $cm^{-2}$ over the hydrogels.

### 2.7 *Fluorescence immunostaining*

To verify fibronectin transfer from patterned glass slides to hydrogels, monoclonal anti-fibronectin produced in mouse (Sigma-Aldrich, St. Louis, MO USA) was diluted at 1:300 in PBS and added to the samples overnight at 4 °C. The solution was then aspirated and rinsed three times with PBS. Alexa Fluor 488 goat anti-mouse IgG (Life Technologies, Grand Island, NY USA) was diluted at 1:1000 in PBS and added for 2 hours at 37 °C. After rinsing three times with PBS, the samples were imaged with an inverted fluorescence microscope (IX81, Olympus, Center Valley, PA USA).

To visualise the morphology of fibroblasts on hydrogel constructs, the cells were fixed and labelled at different time points. For fixation, samples were rinsed with PBS and incubated in 4% paraformaldehyde (PFA, Sigma-Aldrich, St. Louis, MO USA) for 30 minutes. After rinsing three times with PBS, a solution of 3,3′-dihexyloxacarbocyanine iodide ($DiOC_6$, Life Technologies) was added at 1:1000 dilution in PBS to stain for a cell's endoplasmic reticulum, vesicle membranes, and mitochondria. Samples were then permeabilised with 0.1% Triton X-100 (Sigma Aldrich) for 10 minutes and blocked with 2.5% bovine serum albumin (BSA) in PBS to prevent non-specific binding. Cell nuclei were stained with a 1:1000 dilution of 2-(4-amidinophenyl)-1H-indole-6-carboxamidine (DAPI, Life Technologies), and actin was stained with a 1:1000 dilution of rhodamine phalloidin (BD Biosciences). Fluorescent images were taken with the inverted fluorescence microscope.

### 2.8 *Fibronectin and acryl-fibronectin transfer to hydrogels*

Image J software (Abramoff *et al.* 2004) was used for analysis of fibronectin, acryl-fibronectin, and cell alignment patterns. Transfer of fibronectin and acryl-fibronectin from glass coverslips to hydrogels were confirmed quantitatively by measuring the pixel intensity of fluorescent images. To calculate pixel intensity values, a line profile was drawn

across the image and grey values were extracted at each point on the line. To determine the integrity and resolution of patterns, line width measurements of μCP glass coverslips and patterned hydrogels were taken. The line profile tool was used to draw horizontal lines perpendicular to patterned lines on 40x images, and the measured line widths were recorded.

### 2.9 *Fast Fourier transform analysis*

Fast Fourier transform (FFT) image processing analysis was previously demonstrated for cell patterning on hydrogels (Millet *et al.* 2011). Briefly, Image J software was used to enhance image contrast, subtract the background, and filter noise from the image. Images were converted to the frequency domain by FFT transformation and rotated 90° to account for the inherent rotation that occurs during transformation. A circle was drawn over the FFT image, and the oval profile plugin was used to radially sum pixel intensities around the circle. A power spectrum was generated based on radially summated values, with 0° correlating to frequencies at 3 o'clock, 90° at 12 o'clock, 180° at 9 o'clock, and 270° at 6 o'clock.

### 2.10 *Cell morphometrics analysis*

The effect of patterning at the cellular level was analysed by observing changes in cell shape, direction of cell elongation, and orientation of nuclei. Post-image processing, a threshold was applied to make a binary image and individual cells were identified. Image J software object tools were used to measure and compare the cell circularity and nuclear orientation. Ten circularity bins of 0.1 intervals were set up, and circularity values between 0 and 1 were placed in each bin (0 being a line and 1 being a circle). Significance was verified with a Student's t-test statistical analysis. Nuclear orientation was measured by using the 'analyse particles' tool to fit an ellipse to threshold images of DAPI-stained nuclei and measuring the angle of the ellipse. Direction and length of cell elongation was determined by measuring the angle and distance from the nucleus to the furthest edge of the actin stained cell.

## 3. Results

### 3.1 *Fibronectin transfer and pattern retention*

To create patterns of proteins on 3D hydrogel constructs, we modified fibronectin molecules with chemically linkable acrylate groups for crosslinking to the backbone of PEGDA hydrogels during photopolymerisation. This simple concept allowed us to utilise the μCP technique to pattern acryl-fibronectin onto hydrogels prepared with the SLA (Figure 1). We confirmed the transfer of acryl-fibronectin from glass coverslips to hydrogels by quantitative analysis of immunofluorescence imaging. Comparison of hydrogels built on glass coverslips with fibronectin (Figure 2A) and acryl-fibronectin (Figure 2B) showed that acryl-fibronectin successfully transferred from the glass coverslip to PEGDA ($M_W$ 3400 $g \cdot mol^{-1}$) hydrogels. The average pixel intensity of acryl-fibronectin on hydrogels was measured at $129 \pm 10.9$, while fibronectin on hydrogels had an average pixel intensity of $2.6 \pm 0.5$ (Figure 2C).

Patterned line widths of 10, 50, and 100 μm on glass coverslips and hydrogels were measured to verify pattern integrity after acryl-fibronectin transfer. Figure 3 shows fluorescent images of patterned lines on glass coverslips and hydrogels. The actual line widths were $11.5 \pm 0.4$ μm, $49.1 \pm 1.8$ μm, and $98.7 \pm 0.60$ μm, respectively, after PDMS stamping on glass coverslips (Figure 3A), and $13.4 \pm 0.5$ μm, $57.3 \pm 0.6$ μm, $110.5 \pm 5.8$ μm, respectively, after acryl-fibronectin transfer to the 3D hydrogel constructs (Figure 3B). Fibronectin transfer did not occur without acrylate groups (Figure 3C). It is well-known that PEGDA ($M_W$ 3400 $g \cdot mol^{-1}$) swells after photopolymerisation and subsequent washing in PBS. This phenomenon caused the measured line widths on the hydrogels to be greater than those on the glass coverslip (Figure 3D). However, the average pixel intensity of fluorescently-labelled acryl-fibronectin patterns on hydrogels did not appear to decrease significantly to the extent that it would affect cell alignment.

### 3.2 *Cell growth and alignment on hydrogels*

NIH/3T3 mouse embryonic fibroblasts were cultured on 3D hydrogel constructs with acryl-fibronectin patterns of unpatterned, 10, 50, and 100 μm wide lines to demonstrate feasibility of cell alignment. The cells rapidly adhered to and began to spread on the line patterns after one hour in culture. Within 24 hours, the cells were activated to proliferate along the line patterns. Figure 4A shows that the cells recognised the acryl-fibronectin patterns and aligned parallel to the lines. As the line spacing decreased from 100 to 10 μm, the number of cells that bridged patterned lines increased. Regardless of cell bridging, the cells continued to align parallel to the lines.

It was evident from the fluorescent images that as line width patterns decreased, alignment of individual cells increased. This was confirmed quantitatively with fast Fourier transform analysis (Figure 4B). Conversion of images to the frequency domain revealed directed fibroblast growth and linear pattern formation. Distinct peaks were seen in the power spectrum of fibroblasts grown on patterned lines of all widths at 0° and 180°. Fibroblasts grown on unpatterned hydrogels lacked these peaks and had more uniformly-scattered spectrums. Furthermore, as

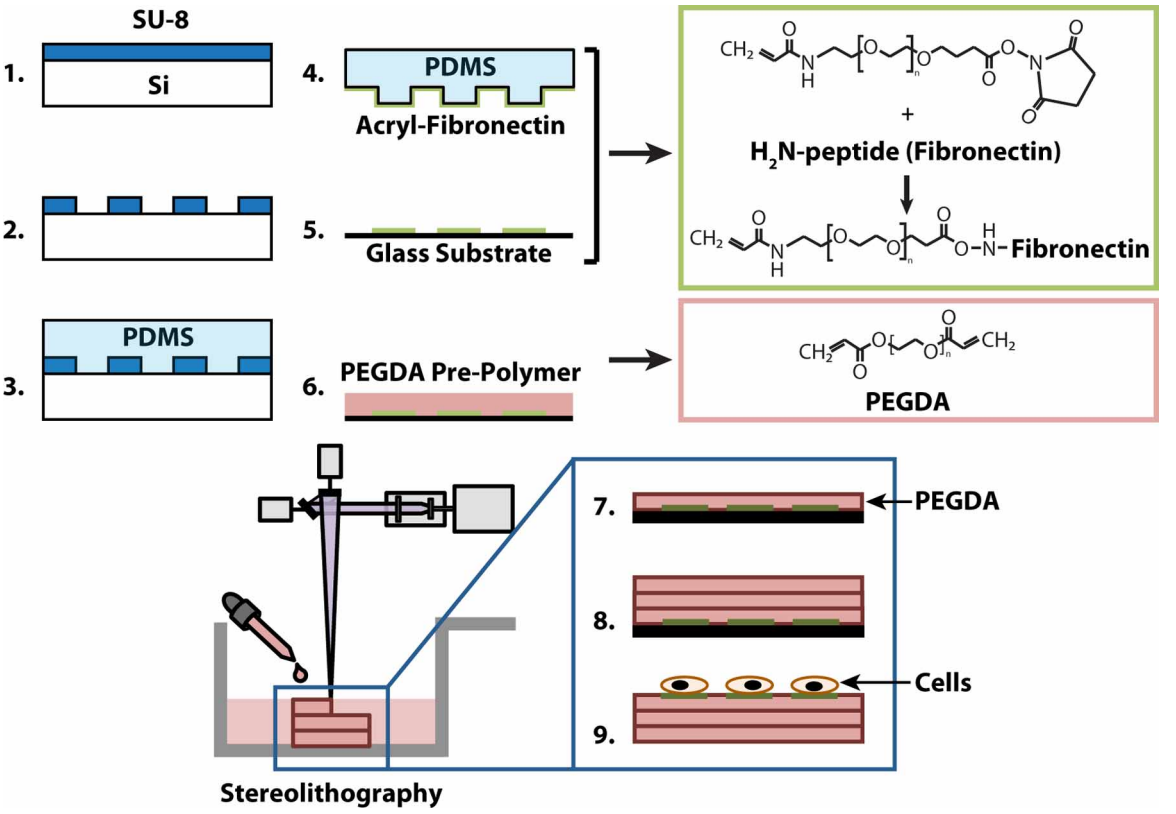


Figure 1. Patterning acryl-fibronectin hydrogels. **(1)** Silicon wafers were coated with 5 μm of SU-8 photoresist. **(2)** Line patterns were formed after exposure of photoresist and silicon with UV light through a chrome mask. **(3)** PDMS was poured over the silicon master and polymerised by baking. A negative of the pattern from the silicon master was imprinted on the surface of the PDMS making a stamp. **(4)** An ink solution containing acryl-fibronectin was pipetted onto the PDMS stamp. Acrylic fibronectin was made by mixing acryl-PEG-NHS and fibronectin in PBS and allowing the PEGDA cross-linker to attach to free lysine groups in fibronectin. **(5)** After stamps were incubated with ink, line patterns were transferred to glass slides by stamping. **(6)** Pre-polymer solution of PEGDA ($M_W$ 3400) and a photoactivator is poured into a dish over patterned glass slides. **(7)** The dish containing pre-polymer and patterned glass is put into the stereolithography apparatus (SLA) and polymerised to form a hydrogel. **(8)** 3D structures were built layer-by-layer adding additional pre-polymer before cross-linking. **(9)** Hydrogels were inverted and seeded with cells. During building of the first layer, acryl-fibronectin was transferred to the surface of the hydrogel allowing for cell attachment.

the line widths increased, the peaks also decreased, and the spectrums were more scattered.

Cell morphometrics were used to examine the individual shape of cells on patterned and unpatterned 3D hydrogel constructs. Growth of cells along the patterned lines altered their shape, making them more linear. Figure 4C shows the decreasing shift of cell circularity measurements between patterned and unpatterned cells. Average circularity was significantly different (Student's t-test, *P*-values = 1.97E-25 and 4.83E-25 for 10 and 50 μm lines, respectively) between unpatterned fibroblasts ($0.41 \pm 0.22$) and fibroblasts restricted to growth on 10 μm ($0.15 \pm 0.10$) and 50 μm ($0.15 \pm 0.11$) lines. Cell shape was altered on 100 μm lines but was not statistically significant.

Figure 5 shows further analysis of the effect of acryl-fibronectin patterns on cell shape and growth. Fibroblast elongation, which was measured from the furthest edge of stained actin on each side of the cell to the nucleus, was parallel to line direction. Average angles were 90.9°, 88.9°, and 89.9° for 10, 50, and 100 μm lines, respectively. Unpatterned fibroblasts had an average angle of 95.4° which was significantly different than patterned fibroblasts (Student's t-test, *P*-values = 4.6E-2, 4.9E-3, and 8.6E-4, respectively). Standard deviations of the average angles were 13.0°, 27.3°, and 48.0° for 10, 50, and 100 μm lines, respectively. Length of elongation caused by patterning showed a significantly greater difference. The average length of extended actin in the cell was 44.33 μm for unpatterned fibroblasts. Patterned cells had average lengths of 78.8, 54.9, and 40.6 μm for 10, 50, and 100 μm lines, respectively (Student's t-test, *P*-values = 9.16E-18, 6.78E-08, and 2.05E-4). The scatter plot in Figure 5A demonstrates

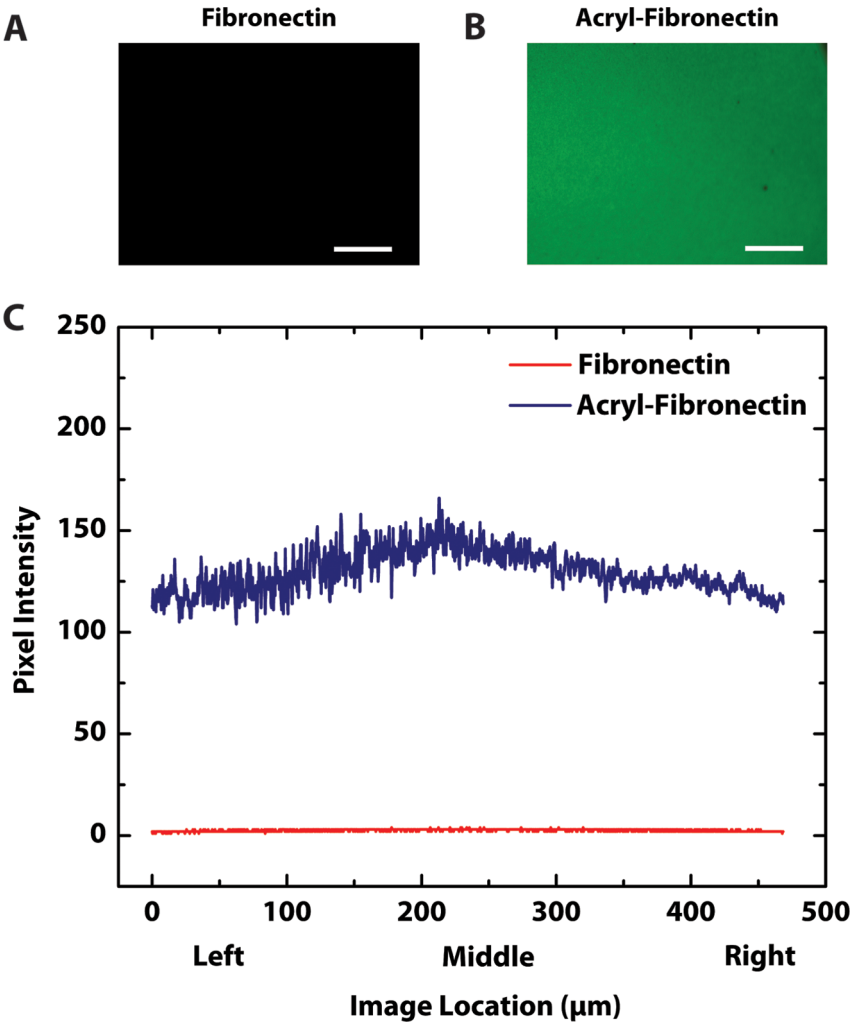


Figure 2. Measuring the transfer of fibronectin and acryl-fibronectin on hydrogels. Hydrogels were fabricated on glass slides with fluorescently-labelled fibronectin and acryl-fibronectin. **(A)** Fluorescent image of a hydrogel fabricated on a glass slide with fibronectin. **(B)** Fluorescent image of a hydrogel built on a slide with acryl-fibronectin. **(C)** Using Image J software, fluorescent intensity of fibronectin and acryl-fibronectin images were extracted and compared. Hydrogels with fibronectin had an average intensity of 2.6, while those with acryl-fibronectin had an average intensity of 129.9. This confirmed that acryl-fibronectin chemically cross-linked fibronectin to the hydrogels.

clustering of the cell elongation around 90° for cells grown on patterns, while the standard deviation plot in Figure 5B shows that the spread of those angles is much smaller with narrower line widths.

## 4. Discussion

Applications for the SLA and other 3D printing platforms using living cells and cell-instructive 3D microenvironments are expanding rapidly. However, none of these enabling technologies are without their drawbacks, and continual development is needed to accommodate the growing number of applications. One of the current limitations of commercial laser-based stereolithographic systems is the minimum feature size required to imitate cell growth and alignment patterns in complex tissue architecture. While photopolymerisable hydrogels can be functionalised with proteins and peptides to enhance cell attachment, it is difficult to pattern them with the SLA at length scales comparable to the cell size. Grooves, microchannels, and other geometrically-restrictive techniques that affect the topology of the hydrogels can alter mechanical properties, which are important in many of these applications. Therefore, micro-contact printing (μCP) offers the capability of directing cell alignment on hydrogel structures without compromising the benefit of creating complex 3D architectures with the SLA. For example, 3D hydrogel cantilevers

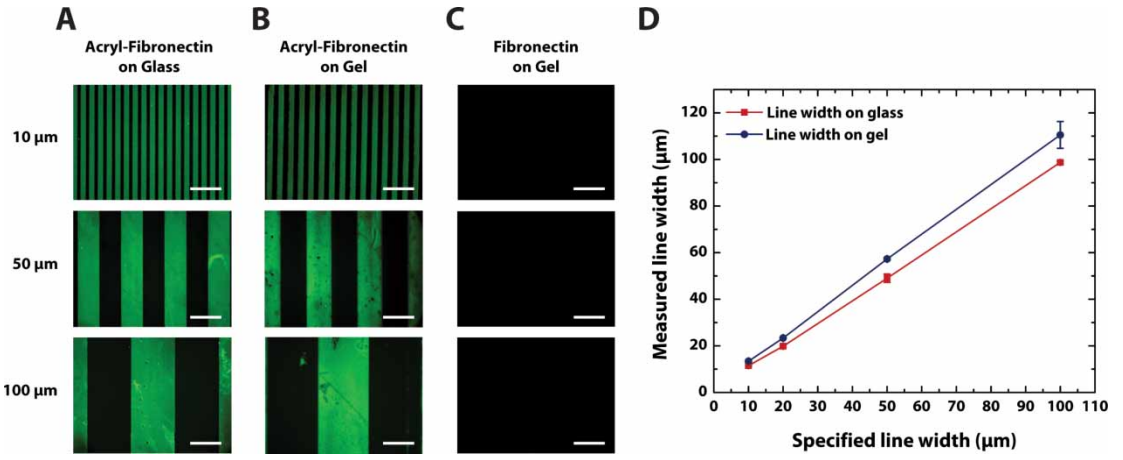


Figure 3. Transferring fibronectin patterns from glass coverslips to hydrogels. **(A)** Glass coverslips with fluorescently-labelled acryl-fibronectin lines 10, 50, and 100 µm wide. **(B)** Hydrogels with fluorescently-labelled acryl-fibronectin lines 10, 50, and 100 µm wide transferred from glass coverslips. **(C)** Hydrogels with fluorescently-labelled fibronectin lines 10, 50, and 100 µm wide (control). **(D)** Comparison of measured line widths on glass coverslips and hydrogels. Scale bars represent 50 µm wide.

fabricated with the SLA can be protein-patterned using our µCP method to align cardiomyocytes for improved actuation force (Chan *et al.* 2012).

Micro-contact printing (µCP) is a well-established technique that does not affect the mechanical properties of hydrogels. It was chosen to pattern acryl-fibronectin in combination with the SLA based on its ease of use, compatible setup, and unrestricted variation in shapes and sizes. Modification of fibronectin with acrylate groups (acryl-fibronectin) was the key component to this method. Without tethered ECM proteins or peptides, PEGDA hydrogels are intrinsically resistant to protein adsorption and cell adhesion. Based on low measured fluorescent intensity, unmodified fibronectin did not transfer to the PEGDA hydrogels (Figure 2A). In contrast, acryl-fibronectin had uniform and high fluorescent intensity throughout the surface of the hydrogels (Figure 2B). This method is not restricted to fibronectin; other proteins or peptides with free lysine ($-NH_3$) groups, such as laminin, collagen, and gelatin, can also be modified with acrylate groups using the same method described.

PEGDA was chosen as the hydrogel material based on its tunable swelling ratio, elastic modulus, and mesh size. It can also be modified for cell-specific adhesion, enzyme-sensitive or hydrolytic degradation, and growth factor-binding signals (Zhu 2010). The swelling ratio and mesh size should be large enough to allow for an adequate supply of oxygen and nutrients, while the elastic modulus and patterning resolution should be high enough for the specific application. Figure 3, which compared the measured line widths on glass coverslips and hydrogels, shows a decrease in the patterning resolution on the PEGDA ($M_W$ 3400 $g \cdot mol^{-1}$) hydrogels. By decreasing the $M_W$ of PEGDA, the patterning resolution can be improved because of the reduced swelling, but this can also affect the organisation and function of cells on the hydrogels.

Although a variety of other configurations are possible, we used line patterns to demonstrate directed cell growth and alignment on the hydrogels. The widths of those line patterns were varied to determine the length scale at which cells would align on the hydrogels. If widths are too thin, cell bodies may be larger than the lines, preventing appropriate cell attachment; if widths are too wide, cells may not recognise the patterns and align to them (Dike *et al.* 1999). Previous findings show that individual cells can recognise lines measuring 5–100 µm wide (Kaji *et al.* 2003). Trends in our data support these findings, with single cells patterning to 10–50 µm wide lines and multiple cells patterning to 100 µm wide lines. In addition, a reduction in circularity can be seen, length of cell elongation, and angle of cell elongation differs between cells grown on patterned lines opposed to unpatterned cells.

Line spacing was also varied to determine length scales at which 'bridging' of cells between patterns occurred. This could prove useful for applications that require cell-cell connections between patterns or formation of cell sheets, without disturbing their alignment. For example, it is known that the complex organisation of cardiac muscle cells and fibroblasts is critical to electrical and mechanical properties in the heart. Because of this, biological cantilevers and actuators cultured with aligned sheets of contractile muscle cells could generate more force than unaligned sheets. Cell bridging would synchronise contraction of the aligned muscle cells and increase density of cells on the devices. However, an optimum line width and spacing would need to be characterised to maximise the performance of the muscle cell sheet. If line spacing was too

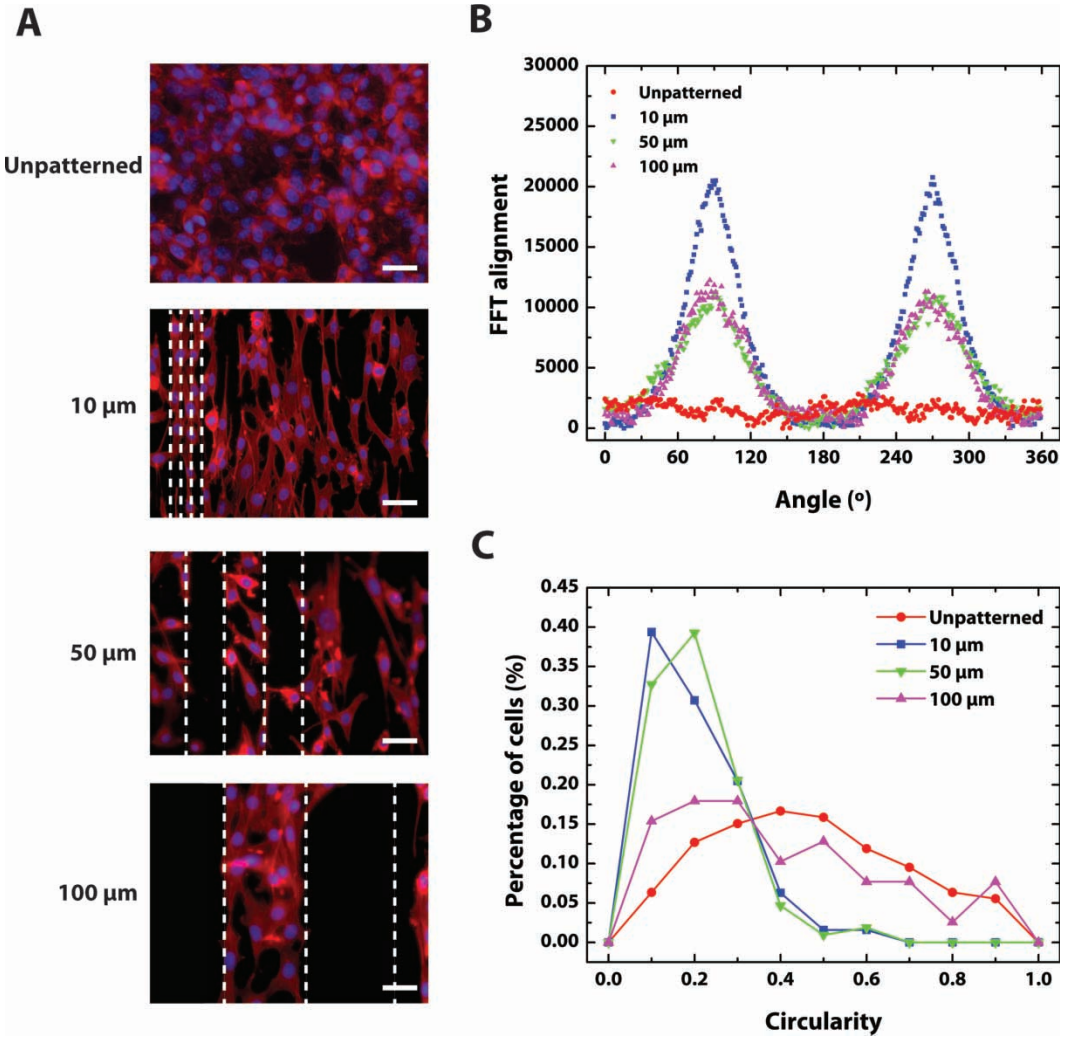


Figure 4. Aligning fibroblasts on unpatterned and patterned hydrogels. **(A)** Fibroblasts with fluorescent nuclear (DAPI) and actin (rhodamine-phalloidin) stains were cultured on hydrogels with unpatterned and patterned acryl-fibronectin with lines 10, 50, and 100 µm wide. **(B)** Power spectrum generated by radially summating frequencies from fast Fourier (FFT) converted images. Peaks at 90° and 180° correspond to vertical alignment in images and can be seen for fibroblasts patterned on lines. **(C)** Analysis of fibroblasts at the cellular level shows a significant decrease in circularity for cells grown on 10 and 50 µm lines. A small but insignificant shift can be seen on 100 µm lines. A decrease in circularity can be attributed to a constriction of cellular growth area. Scale bars represent 50 µm wide.

small, cells may not be restricted to the acryl-fibronectin patterns and align properly on the hydrogels.

Other biological applications that study co-cultures and emerging behaviours of cells can benefit from this method. Motor neurons can be directed to align and interact with contractile muscle cells to form functional neuromuscular junctions (NMJ) (Guo *et al.* 2011). These motor neuron and muscle co-cultures can be used as *in vitro* models to understand NMJ-related pathogenesis, drug discovery, and even creation of cellular machines that utilise the sensing and actuation capabilities of the two cell types. This method can also be directly employed to study stem cell niches based on various physical properties, such as cellular organisation and matrix elasticity (Paik *et al.* 2012). Organised cell alignment is critical to controlling tissue architecture and biological function. Overall, there are numerous future experiments and applications that can be explored with the ability to design 3D hydrogel substrates that can support, pattern, and harness the outputs of multiple cell types.

## 5. Conclusion

We have demonstrated a simple method for patterning and aligning living cells on hydrogel substrates by combining

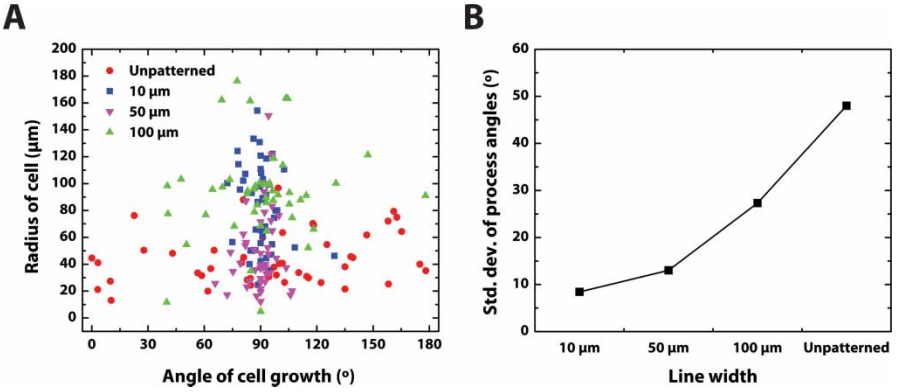


Figure 5. Measuring direction of cell elongation of fibroblasts. **(A)** Cell elongation and direction were measured by drawing a line from the nucleus to the furthest extended edge of the cell. Scatter distribution shows clustering of cell elongation near 90° for fibroblasts grown on 10 and 50 µm lines. Unpatterned cells were significantly different in both elongation and uniform distribution of edge direction. **(B)** Standard deviation of angle values for cell process alignment shows smaller spread values for narrower line widths, which demonstrates higher alignment of cells.

the micro-contact printing (µCP) technique with the stereolithographic process. The key component of this method was acryl-fibronectin, which could be patterned onto glass surfaces and transferred to photopolymerisable PEGDA hydrogels. NIH/3T3 mouse embryonic fibroblasts were cultured on hydrogels patterned with acryl-fibronectin of various line widths. While resolution of the line widths depended on swelling ratios of the hydrogels, it did not visibly affect cell attachment or alignment on the patterns. Analysis of cells cultured on the hydrogels showed cells spreading and growing parallel to the direction of the lines. Cell 'bridging' occurred between patterns and increased as line spacing decreased. Overall, µCP can be used to enhance cell-based applications with the SLA by patterning proteins of various shapes and size on photopolymerisable hydrogels for directed cell growth and alignment. It can be used to increase hierarchical organisation of cells in engineered biohybrid systems, or to expand our understanding of developmental biology and the mechanism of diseases.

## Acknowledgements

We thank Elise Corbin for her help with figures. This project was funded by the National Science Foundation (NSF), Science and Technology Center (STC) and Emerging Behaviors in Integrated Cellular Systems (EBICS) Grant CBET-0939511 (R.B. and H.K.) and by a cooperative agreement that was awarded to University of Illinois at Urbana-Champaign (UIUC) and administered by the U.S. Army Medical Research & Materiel Command (USAMRMC) and the Telemedicine & Advanced Technology Research Center (TATRC), under Contract #: W81XWH0810701.

## References

Abramoff, M.D., Magalhaes, P.J. and Ram, S.J., 2004. Image processing with ImageJ. *Biophotonics International*, **11** (7), 36–42.

Arcaute, K., Mann, B.K. and Wicker, R.B., 2006. Stereolithography of three-dimensional bioactive poly(ethylene glycol) constructs with encapsulated cells. *Annals of Biomedical Engineering*, **34** (9), 1429–1441.

Aubin, H., et al., 2010. Directed 3D cell alignment and elongation in microengineered hydrogels. *Biomaterials*, **31** (27), 6941–6951.

Barker, T.M., Earwaker, W.J. and Lisle, D.A., 1994. Accuracy of stereolithographic models of human anatomy. *Australasian Radiology*, **38** (2), 106–111.

Bott, K., et al., 2010. The effect of matrix characteristics on fibroblast proliferation in 3D gels. *Biomaterials*, **31** (32), 8454–8464.

Buxboim, A., Ivanovska, I.L. and Discher, D.E., 2010. Matrix elasticity, cytoskeletal forces and physics of the nucleus: How deeply do cells "feel" outside and in? *Journal of Cell Science*, **123** (Pt 3), 297–308.

Chan, V., et al., 2010. Three-dimensional photopatterning of hydrogels using stereolithography for long-term cell encapsulation. *Lab on a Chip*, **10** (16), 2062–2070.

Chan, V., et al., 2012. Multi-material bio-fabrication of hydrogel cantilevers and actuators with stereolithography. *Lab on a Chip*, **12** (1), 88–98.

Charest, J.L., et al., 2006. Combined microscale mechanical topography and chemical patterns on polymer cell culture substrates. *Biomaterials*, **27** (11), 2487–2494.

Chen, C.S., et al., 1998. Micropatterned surfaces for control of cell shape, position, and function. *Biotechnology Progress*, **14** (3), 356–363.

Cooke, M.N., et al., 2003. Use of stereolithography to manufacture critical-sized 3D biodegradable scaffolds for bone ingrowth. *Journal of Biomedical Materials Research. Part B, Applied Biomaterials*, **64** (2), 65–69.

Dike, L.E., et al., 1999. Geometric control of switching between growth, apoptosis, and differentiation during angiogenesis using micropatterned substrates. *In Vitro Cellular and Developmental Biology - Animal*, **35** (8), 441–448.

Discher, D.E., Janmey, P. and Wang, Y.L., 2005. Tissue cells feel and respond to the stiffness of their substrate. *Science*, **310** (5751), 1139–1143.

Engler, A.J., et al., 2006. Matrix elasticity directs stem cell lineage specification. *Cell*, **126** (4), 677–689.

Geiger, B., Spatz, J.P. and Bershadsky, A.D., 2009. Environmental sensing through focal adhesions. *Nature Reviews Molecular Cell Biology*, **10** (1), 21–33.

Guillame-Gentil, O., et al., 2010. Engineering the extracellular environment: Strategies for building 2D and 3D cellular structures. *Advanced Materials*, **22** (48), 5443–5462.

Guo, X., et al., 2011. Neuromuscular junction formation between human stem cell-derived motoneurons and human skeletal muscle in a defined system. *Biomaterials*, **32** (36), 9602–9611.

Hadjipanayi, E., Mudera, V. and Brown, R.A., 2009. Guiding cell migration in 3D: A collagen matrix with graded directional stiffness. *Cell Motility and the Cytoskeleton*, **66** (3), 121–128.

Ifkovits, J.L. and Burdick, J.A., 2007. Review: Photopolymerizable and degradable biomaterials for tissue engineering applications. *Tissue Engineering*, **13** (10), 2369–2385.

Jabbari, E., 2011. Bioconjugation of hydrogels for tissue engineering. *Current Opinion in Biotechnology*, **22** (5), 655–660.

Jacobs, P.F., 1992. *Rapid prototyping and manufacturing: Fundamentals of stereolithography*. Dearborn, MI: Society of Manufacturing Engineers.

Jeong, J.H., et al., 2012. ''Living'' microvascular stamp for patterning of functional neovessels; orchestrated control of matrix property and geometry. *Advanced Materials*, **24** (1), 58–63.

Kaji, H., et al., 2003. Intracellular Ca2+ imaging for micropatterned cardiac myocytes. *Biotechnology and Bioengineering*, **81** (6), 748–751.

Kane, R.S., et al., 1999. Patterning proteins and cells using soft lithography. *Biomaterials*, **20** (23–24), 2363–2376.

Khetan, S. and Burdick, J.A., 2011. Patterning hydrogels in three dimensions towards controlling cellular interactions. *Soft Matter*, **7** (3), 830–838.

Kim, J., et al., 2007. Establishment of a fabrication method for a long-term actuated hybrid cell robot. *Lab on a Chip*, **7** (11), 1504–1508.

Lee, S.-H., Moon, J.J. and West, J.L., 2008. Three-dimensional micropatterning of bioactive hydrogels via two-photon laser scanning photolithography for guided 3D cell migration. *Biomaterials*, **29** (20), 2962–2968.

McDevitt, T., Angello, J. and Whitney, M., 2002. In vitro generation of differentiated cardiac myofibers on micropatterned laminin surfaces. *Journal of Biomedical Materials Research*, **60** (3), 472–479.

Melchels, F., Feijen, J. and Grijpma, D.W., 2010. A review on stereolithography and its applications in biomedical engineering. *Biomaterials*, **31** (24), 6121–6130.

Melchels, F., et al., 2011. CAD/CAM-assisted breast reconstruction. *Biofabrication*, **3** (3), 034114.

Melchels, F. et al., 2012. Additive manufacturing of tissues and organs. *Progress in Polymer Science*, **37** (8), 1079–1104

Millet, L.J., et al., 2011. Pattern analysis and spatial distribution of neurons in culture. *Integrative Biology*, **3** (12), 1167–1178.

Nguyen, K.T. and West, J.L., 2002. Photopolymerizable hydrogels for tissue engineering applications. *Biomaterials*, **23** (22), 4307–4314.

Paik, I. et al., 2012. Rapid micropatterning of cell lines and human pluripotent stem cells on elastomeric membranes. *Biotechnology and Bioengineering*, April 17. http://onlinelibrary.wiley.com/doi/10.1002/bit.24529/abstract [Epub ahead of print]

Park, J., et al., 2006. Fabrication of complex 3D polymer structures for cell–polymer hybrid systems. *Journal of Micromechanics and Microengineering*, **16** (8), 1614–1619.

Parker, K.K., et al., 2002. Directional control of lamellipodia extension by constraining cell shape and orienting cell tractional forces. *FASEB Journal*, **16** (10), 1195–1204.

Reinhart-King, C.A, Dembo, M. and Hammer, D.A., 2008. Cell-cell mechanical communication through compliant substrates. *Biophysical Journal*, **95** (12), 6044–6051.

Sarig-Nadir, O., et al., 2009. Laser photoablation of guidance microchannels into hydrogels directs cell growth in three dimensions. *Biophysical Journal*, **96** (11), 4743–4752.

Seitz, H., et al., 2005. Three-dimensional printing of porous ceramic scaffolds for bone tissue engineering. *Journal of Biomedical Materials Research. Part B, Applied Biomaterials*, **74** (2), 782–788.

Sodian, R., et al., 2002. Application of stereolithography for scaffold fabrication for tissue engineered heart valves. *ASAIO Journal*, **48** (1), 12–16.

Tibbitt, M.W. and Anseth, K.S., 2009. Hydrogels as extracellular matrix mimics for 3D cell culture. *Biotechnology and Bioengineering*, **103** (4), 655–663.

Vogel, V. and Sheetz, M., 2006. Local force and geometry sensing regulate cell functions. *Nature Reviews Molecular Cell Biology*, **7** (4), 265–275.

West, J.L., 2011. Protein-patterned hydrogels: Customized cell microenvironments. *Nature Materials*, **10** (10), 727–729.

Winder, J. and Bibb, R., 2005. Medical rapid prototyping technologies: State of the art and current limitations for application in oral and maxillofacial surgery. *Journal of Oral and Maxillofacial Surgery*, **63** (7), 1006–1015.

Wong, J.Y., Leach, J.B. and Brown, X.Q., 2004. Balance of chemistry, topography, and mechanics at the cell–biomaterial interface: Issues and challenges for assessing the role of substrate mechanics on cell response. *Surface Science*, **570** (1–2), 119–133.

Zhu, J., 2010. Bioactive modification of poly (ethylene glycol) hydrogels for tissue engineering. *Biomaterials*, **31** (17), 4639–4656.

Zorlutuna, P., et al., 2011. Stereolithography-based hydrogel microenvironments to examine cellular interactions. *Advanced Functional Materials*, **21** (19), 3642–3651.